Spatial Statistics 53 (2023) 100720

Contents lists available at ScienceDirect

Spatial Statistics

journal homepage: www.elsevier.com/locate/spasta

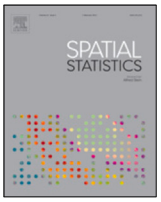

Mapping the short-term exposure–response relationships between environmental factors and health outcomes and identifying the causes of heterogeneity: A multivariate-conditional-meta-autoregression-based two-stage strategy☆

Wei Wang [a], Fang Liao [b,c], Fei Yin [a], Yue Ma [a,d,*]

[a] West China School of Public Health and West China Fourth Hospital, Sichuan University, China
[b] Sichuan Provincial Center for Mental Health, Sichuan Academy of Medical Sciences & Sichuan Provincial People's Hospital, Chengdu, 610072, China
[c] Key Laboratory of psychosomatic medicine, Chinese Academy of Medical Sciences, Chengdu 610072, China
[d] Institute of Systems Epidemiology, West China School of Public Health and West China Fourth Hospital, Sichuan University, China

ARTICLE INFO

Article history:
Received 18 September 2022
Received in revised form 7 November 2022
Accepted 7 December 2022
Available online 12 December 2022

Keywords:
Spatial distribution
Exposure–response association
Multivariate meta-regression
Two-stage strategy
Conditional autoregression

ABSTRACT

Studying the spatial distribution of short-term exposure–response relationships (ERRs) between environmental factors and health-related outcomes and identifying the causes of spatial heterogeneity are of great importance on making region-specific environment-related public health policies. However, the widely used multivariate meta-regression (MMR)-based two-stage strategy does not consider the spatial dependence between regions, which may give unsatisfactory results, even a false policy implication. More importantly, possibly due to the limitation, the spatial distribution of short-term ERRs is less frequently focused on. In this work, we combined the conditional autoregression with MMR to construct an extended model called MCMAR. Then a MCMAR-based two-stage strategy is developed to map the

☆ Acknowledgments: The authors would like to thank Xiong Xiao for providing the city-specific ERRs from the first stage in the motivating example. This work was supported by the National Natural Science Foundation of China under Grant 81803332, the National Natural Science Foundation of China under Grant 81872713, and the Sichuan Science & Technology Program, China under Grant 2021YFS0181. Mourn my father and hope him rest in peace.

* Corresponding author.
E-mail address: gordonrozen@scu.edu.cn (Y. Ma).

https://doi.org/10.1016/j.spasta.2022.100720

ERRs and identify the causes of heterogeneity. A published motivating example and a simulation study were used to validate the efficiency of our strategy. Results show that the MCMAR-based strategy achieved considerably better fit performance in terms of the Akaike information criterion, obtained a more reasonable spatial distribution of ERRs, and identified more accurate causes of heterogeneity than the classic strategy. As numerous spatial ERR datasets have been and are being produced, we believed that MCMAR-based two-stagy strategy will have an important and wide application value.

1. Introduction

In the last few decades, with the improvement in environmental monitoring systems and disease surveillance systems, a large number of time-series studies have been carried out to characterize the exposure–response relationships (ERRs) between environmental risk factors and health-related outcomes (Shah et al., 2013; Katsouyanni et al., 1997; Shang et al., 2013; Newell et al., 2017; Requia et al., 2018). Due to the distinctions in culture, natural conditions, economic levels and sanitary conditions, different regions often present heterogeneous ERRs. For example, Shah et al.'s (Shah et al., 2015) study shows a stronger association between air pollution and stroke in low-income countries. Tian et al.'s (Tian et al., 2019) study shows a stronger association between air pollution and cardiovascular disease-related hospital admission in central south, eastern, and northern Chinese cities, and temperature and humidity significantly modify the association. Studying such heterogeneity of ERRs among different regions, including but not limited to characterizing region-specific ERRs (i.e., characterizing the spatial distribution of ERRs), synthesizing heterogeneous ERRs, and identifying the causes of heterogeneity, assists in (1) making reasonable region-specific public health interventions, (2) constructing region-specific early warning systems, (3) assessing the environment-related attributable disease burden, and (4) identifying high-risk effect-modifying factors and high-sensitivity risk region. These items play important roles on making cost-effective environment-related policies, for example, decreasing the exposure to certain environment factor is more cost-effective in the regions with high-sensitivity risk.

Currently, the two-stage strategy has become the main tool for investigating (or dealing with) the heterogeneity of ERRs since Gasparrini et al.'s work (Gasparrini et al., 2012). In the first stage, common region-stratified time-series regression models with the same model forms, such as general linear models, generalized linear models, and generalized additive models (GAMs), are used to obtain rough region-specific ERR estimations. When the ERR presents nonlinear and even lag effects, which frequently occur in environmental risk factors due to complex pathogenic mechanisms, the ERR is defined by multiple parameters (i.e., a vector) commonly estimated by a GAM, such as a distributed lag nonlinear model (DLNM) (Gasparrini et al., 2010; Gasparrini, 2014). In the second stage, meta-analysis (or meta-regression), hereafter MR, is used to pool the estimations for more accurate average and region-specific estimations as well as to explore the causes of heterogeneity by incorporating the region-level predictors into the model. When the ERR is defined by multiple parameters, multivariate MR (MMR) is used as the replacement. As MR is a special case of MMR, to write with brevity, we use MMR to represent MR and MMR. With its flexibility in adjusting confounders and characterizing complex ERRs in the first stage, the MMR-based two-stage strategy has been widely used in epidemiological studies.

However, MMR in the second stage does not consider commonly existing spatial autocorrelation (Tobler, 1970), i.e., two regions closer together are more related to each other. Previous studies Anselin (1988), Zadnik and Reich (2006) have shown that ignoring spatial autocorrelation will lead to a loss of model performance, possibly increasing false positive error and decreasing

predictive ability. Therefore, the MMR-based two-stage strategy is likely to falsely identify the causes of heterogeneity and obtain an inaccurate spatial distribution of heterogeneous ERRs, which may provide a false implication for public health intervention. Introducing spatial autocorrelation may have the potential to further elevate the performance of the classic two-stage strategy. More notably, due to not considering the spatial distribution, the MMR-based strategy is less frequently used to map the ERRs. The ideal Bayesian spatiotemporal model will cost unacceptably intensive computation sources due to the complex confounders and the long time series. With the lack of efficient tools, it is of great application value to develop a method to accurately map the short-term ERRs and identify the causes of heterogeneity.

Since Besag et al.'s work (Besag et al., 1991), the conditional autoregression (CAR) model has been the rule used to characterize the spatial distribution of risks in disease mapping, but the CAR model focused on the observed raw data without estimation error rather than the estimated data with standard error, such as the ERR estimations from the first stage, which are of interest in meta-regression. Some meta-regressions have been developed to consider the autocorrelations between observed values (Hedges and Olkin, 1985; Viechtbauer, 2010), but they are neither available for multivariate response values, nor make full use of the common CAR-based spatial structure, especially the more flexible Leroux CAR prior. In this work, by combining the CAR with multivariate meta-regression, an extended model, called multivariate conditional meta autoregression (MCMAR), was constructed. Univariate conditional meta autoregression, as a special case of MCMAR, is not mentioned here for brevity. By using MCMAR to substitute MMR in the second stage, a novel MCMAR-based two-stage strategy can be used to improve the performance of the MMR-based two-stage strategy. In Section 2, the methodology regarding MCMAR is detailed. In Section 3, a published motivating example is used to illustrate the application of the MCMAR-based two-stage strategy in mapping the complex heterogeneous ERRs and exploring the causes of such heterogeneity. In Section 4, a simulation study is used to verify the advantage of MCMAR over MMR. Section 5 presents a general discussion.

2. Methods

In this section, based on the region-specific ERRs estimated by GAMs in the first stage, we detailed the methodology of MCMAR. The MCMAR-based two-stage strategy can be easily derived, seen in Section 3.

2.1. Model structure of MCMAR

The ERR for each region is defined by a k-dimensional vector along with its covariance, which usually comes from the first-stage model and the details can be found in Section 3.3. We set a total of m regions. $\hat{\boldsymbol{\theta}}_i$ is a k-dimensional vector defining the estimated ERR in region i from the first stage. $\mathbf{S}_i$ is the covariance of $\hat{\boldsymbol{\theta}}_i$. $\boldsymbol{\theta}_i$ defines the unknown real ERR. Then,

$$\hat{\boldsymbol{\theta}}_i|\boldsymbol{\theta}_i \sim MN\left(\boldsymbol{\theta}_i, \mathbf{S}_i\right), \tag{1}$$

where $MN(\cdot)$ is the multivariate normal distribution. The incorporated region-level predictors in region i are indicated by a p-dimension vector $\boldsymbol{x}_i$ with the first element of one as the intercept. We define

$$\mathbf{X}_i = \mathbf{I}_k \otimes \boldsymbol{x}_i^T = \begin{bmatrix} \boldsymbol{x}_i^T & \mathbf{0} & \cdots & \mathbf{0} \\ \mathbf{0} & \boldsymbol{x}_i^T & & \mathbf{0} \\ \vdots & & \ddots & \vdots \\ \mathbf{0} & \mathbf{0} & \cdots & \boldsymbol{x}_i^T \end{bmatrix},$$

where $\mathbf{I}_k$ is a $k \times k$ identity matrix and $\otimes$ is the Kronecker product. Then, $\boldsymbol{\theta}_i$ can be formulized as

$$\boldsymbol{\theta}_i = \mathbf{X}_i\boldsymbol{\beta} + \boldsymbol{\xi}_i,$$

where $\boldsymbol{\beta}$ is a pk-dimensional regression coefficient vector defining the association of predictors with ERR. $\boldsymbol{\xi}_i$ is a k-dimensional random effect vector defining the region-specific heterogeneous

component that cannot be explained by region-level predictors. Thus, Model (1) can be written as follows:

$$\begin{aligned} &\hat{\boldsymbol{\theta}}_i = \mathbf{X}_i\boldsymbol{\beta} + \boldsymbol{\xi}_i + \boldsymbol{\varepsilon}_i \\ &\boldsymbol{\varepsilon}_i \sim MN\left(\mathbf{0}, \mathbf{S}_i\right), \boldsymbol{\varepsilon}_i \perp \boldsymbol{\xi}_i \end{aligned} \tag{2}$$

where $\perp$ is a symbol indicating independence between two random variables. In MMR, $\boldsymbol{\xi}_i$ and $\boldsymbol{\xi}_j$, with $i \neq j$, are independent and identically distributed. In this work, we broke the independence condition and introduced spatial autocorrelation to construct the MCMAR model.

Letting $\boldsymbol{\xi}_i$ be the ith column vector of the $k \times m$ matrix $\boldsymbol{\xi}$, we specify

$$\boldsymbol{\xi} \sim \mathcal{MN}\left(\mathbf{0}, \mathbf{V}, \mathbf{U}\right), \tag{3}$$

where $\mathcal{MN}(\cdot)$ is the matrix normal distribution. $\mathbf{V}$ is a $k \times k$ matrix defining the correlation among rows, i.e., the correlation among the elements in $\boldsymbol{\theta}_i$. $\mathbf{U}$ is a $m \times m$ matrix defining the correlation among columns, i.e., the spatial autocorrelation. Furthermore, let $\boldsymbol{\varepsilon}_i$ and $\hat{\boldsymbol{\theta}}_i$ be the ith column vector of $k \times m$ matrix $\boldsymbol{\varepsilon}$ and $\hat{\boldsymbol{\theta}}$, respectively, and let

$$\begin{aligned} &\mathbf{X}^* = \begin{bmatrix} \mathbf{X}_1 \\ \mathbf{X}_2 \\ \vdots \\ \mathbf{X}_m \end{bmatrix}, \mathbf{D} = \begin{bmatrix} \mathbf{S}_1 & \mathbf{0} & \cdots & \mathbf{0} \\ \mathbf{0} & \mathbf{S}_2 & & \mathbf{0} \\ \vdots & & \ddots & \vdots \\ \mathbf{0} & \mathbf{0} & \cdots & \mathbf{S}_m \end{bmatrix}, \\ &\boldsymbol{\xi}^* = \mathrm{vec}\left(\boldsymbol{\xi}\right), \boldsymbol{\varepsilon}^* = \mathrm{vec}\left(\boldsymbol{\varepsilon}\right), \hat{\boldsymbol{\theta}}^* = \mathrm{vec}\left(\hat{\boldsymbol{\theta}}\right), \end{aligned}$$

where $\mathrm{vec}\left(\cdot\right)$ indicates vectorizing a matrix according to its column vectors. Combining Formulas (2) and (3), we constructed MCMAR as follows:

$$\begin{aligned} &\hat{\boldsymbol{\theta}}^* = \mathbf{X}^*\boldsymbol{\beta} + \boldsymbol{\xi}^* + \boldsymbol{\varepsilon}^*, \\ &\boldsymbol{\xi}^* \sim MN\left(\mathbf{0}, \mathbf{U} \otimes \mathbf{V}\right), \boldsymbol{\varepsilon}^* \sim MN\left(\mathbf{0}, \mathbf{D}\right), \boldsymbol{\xi}^* \perp \boldsymbol{\varepsilon}^*. \end{aligned} \tag{4}$$

Then,

$$\hat{\boldsymbol{\theta}}^* \sim MN\left(\mathbf{X}^*\boldsymbol{\beta}, \mathbf{U} \otimes \mathbf{V} + \mathbf{D}\right). \tag{5}$$

As Leroux prior-based conditional autoregression (LCAR) (Leroux et al., 2000) has been commonly used to address the spatial autocorrelation issue due to its efficient computation and flexibility in considering both structured and unstructured random effects, according to the Leroux prior, we defined $\mathbf{U}$ as follows:

$$\mathbf{U} = \sigma^2\left[\rho\mathbf{R} + \left(1-\rho\right)\mathbf{I}_m\right]^{-\mathbf{1}},$$

where σ^2 is the variance parameter. $\mathbf{R}$ reflecting the structured random effect is a $m \times m$ symmetric matrix with elements:

$$\mathbf{R}_{ij} = \begin{cases} \mathcal{N}_i, & i = j \\ -I(i \sim j), & i \neq j, \end{cases}$$

where $\mathcal{N}_i$ indicates the number of neighbors around the ith region, $i \sim j$ indicates that regions i and j are neighbors, and $I(\cdot)$ is the indicator function. Identity matrix $\mathbf{I}_m$ reflects the unstructured random effect. ρ balances the intensity between structured and unstructured random effects. When $\rho = 0$, MCMAR becomes MMR. When $\rho \neq 0$, an intuitive explanation can be presented as follows:

$$\boldsymbol{\xi}_i | \boldsymbol{\xi}_{-i} \sim MN\left(\frac{\rho}{1-\rho+\rho\mathcal{N}_i}\sum_{j\sim i}\boldsymbol{\xi}_j, \frac{\sigma^2\mathbf{V}}{\mathcal{N}_i}\right), \tag{6}$$

where $\boldsymbol{\xi}_i$ is the random effect vector in region i and $\boldsymbol{\xi}_{-i}$ is the random effect matrix in all the regions with the ith region deleted. For $\mathbf{V}$, without any prior, an unstructured $k \times k$ symmetric matrix is defined, i.e., with $k(k+1)/2$ parameters to be estimated.

2.2. Parameter estimation

At present, various estimation methods have been well developed to estimate the parameters for MMR, such as likelihood-based methods, multivariate moment methods, estimating equations, Bayesian approaches, and iterative generalized least squares, in which likelihood-based methods have been frequently used since the release of the R package "mvmeta". For the LCAR model, the Bayesian approach is the mainstream method. In this work, to enhance the comparison between MCMAR and MMR implemented by "mvmeta", we used the maximum likelihood (ML) and restricted maximal likelihood (REML) methods to estimate the parameters in MCMAR.

According to Formula (5), the log-likelihood of MCMAR can be written as

$$LL\left(\boldsymbol{\beta}, \mathbf{U}, \mathbf{V}|\hat{\boldsymbol{\theta}}^*, \mathbf{X}^*, \mathbf{D}\right) = -\frac{mk}{2}\ln(2\pi) - \frac{1}{2}\ln(|\boldsymbol{\Sigma}|) - \frac{1}{2}\left[\hat{\boldsymbol{\theta}}^* - \mathbf{X}^*\boldsymbol{\beta}\right]^{\mathrm{T}}\boldsymbol{\Sigma}^{-1}\left[\boldsymbol{y}^* - \mathbf{X}^*\boldsymbol{\beta}\right] \tag{7}$$

where $\boldsymbol{\Sigma} = \mathbf{U} \otimes \mathbf{V} + \mathbf{D}$. When $\mathbf{U}$ and $\mathbf{V}$ are known, i.e., $\boldsymbol{\Sigma}$ is known, the ML estimators can be expressed using closed-form equations as follows:

$$\hat{\boldsymbol{\beta}} = \left[\mathbf{X}^{*\mathrm{T}}\boldsymbol{\Sigma}^{-1}\mathbf{X}^*\right]^{-1}\mathbf{X}^{*\mathrm{T}}\boldsymbol{\Sigma}^{-1}\hat{\boldsymbol{\theta}}^*, \tag{8}$$

$$\mathrm{cov}\left(\hat{\boldsymbol{\beta}}\right) = \left[\mathbf{X}^{*\mathrm{T}}\boldsymbol{\Sigma}^{-1}\mathbf{X}^*\right]^{-1}, \tag{9}$$

which are also generalized least square estimators. When $\boldsymbol{\Sigma}$ is unknown, an iterative method is needed to acquire the estimations of $\boldsymbol{\beta}$, $\mathbf{U}$ and $\mathbf{V}$ by maximizing the joint log-likelihood function in (7). As the ML estimator for covariance parameters does not consider the loss of degrees of freedom from the fixed parameter of $\boldsymbol{\beta}$, it will bias the estimations of $\mathbf{U}$ and $\mathbf{V}$, thus biasing the estimations of $\boldsymbol{\xi}^*$ and $\boldsymbol{\beta}$. The REML method is an alternative that can obtain unbiased estimations by maximizing an adjusted log-likelihood function when estimating $\mathbf{U}$ and $\mathbf{V}$. The adjusted log-likelihood function is based on $(m-p)\,k$ linearly independent error contrasts rather than the full data vector $\hat{\boldsymbol{\theta}}^*$ and is expressed as follows:

$$RLL\left(\mathbf{U}, \mathbf{V}|\hat{\boldsymbol{\theta}}^*, \mathbf{X}^*, \mathbf{D}\right) = -\frac{(m-p)\,k}{2}\ln(2\pi) - \frac{1}{2}\ln(|\boldsymbol{\Sigma}|) - \frac{1}{2}\ln\left|\mathbf{X}^{*\mathrm{T}}\boldsymbol{\Sigma}^{-1}\mathbf{X}^*\right|$$

$$-\frac{1}{2}\left[\boldsymbol{y}^* - \mathbf{X}^*\hat{\boldsymbol{\beta}}\right]^{\mathrm{T}}\boldsymbol{\Sigma}^{-1}\left[\boldsymbol{y}^* - \mathbf{X}^*\hat{\boldsymbol{\beta}}\right] \tag{10}$$

where $\hat{\boldsymbol{\beta}}$ is defined in Eq. (8).

To guarantee that $\mathbf{V}$ and $\mathbf{U}$ are always positive definite in the iterative processes, we used Cholesky decomposition to define $\mathbf{V}$, i.e., $\mathbf{V} = \mathbf{G}^{\mathrm{T}}\mathbf{G}$, where $\mathbf{G}$ is an upper triangular matrix with $k(k+1)/2$ parameters that need to be estimated. $\mathbf{U}$ can be written as $\mathbf{U} = \sigma^2\left(\mathbf{I}_n - \rho\mathbf{C}\right)^{-1}$, where $\mathbf{C} = \mathbf{I}_n - \mathbf{R}$. Then, $\mathbf{U}$ and $\mathbf{C}$ have the same eigenvectors. Let $\mathbf{E}$ be an orthogonal matrix composed of the eigenvectors of $\mathbf{C}$, and $\mathbf{D}_{\boldsymbol{\lambda}}$ be the diagonal matrix of the corresponding eigenvalues vector $\boldsymbol{\lambda} = \{\lambda_i\}$, i.e., the spectral decomposition of $\mathbf{C}$ can be expressed as $\mathbf{C} = \mathbf{E}\mathbf{D}_{\boldsymbol{\lambda}}\mathbf{E}^{\mathrm{T}}$. Thus, the spectral decomposition of $\mathbf{U}$ can be written as $\mathbf{U} = \sigma^2\mathbf{E}\left(\mathbf{I}_n - \rho\mathbf{D}_{\boldsymbol{\lambda}}\right)^{-1}\mathbf{E}^{\mathrm{T}}$. We defined $\rho \in (\rho_L, \rho_U)$, and then ρ_L and ρ_U can be easily derived by limiting $\frac{1}{1-\rho\lambda_i} > 0$ for every i to make $\mathbf{U}$ positive definite. To make the model identifiable, we set $\sigma^2 = 1$ and $\sum_{i=1}^{m}\boldsymbol{\xi}_i = \mathbf{0}$. The iterative algorithm can be summarized as follows:

The ML- or REML-based iterative algorithm for MCMAR

0. Use $\mathbf{G}$ and ρ to define $\mathbf{V}$ and $\mathbf{U}$, respectively. Set $\mathbf{V} = \mathbf{G}^{\mathrm{T}}\mathbf{G}$ and calculate the range of ρ, i.e., $\rho \in (\rho_L, \rho_U)$.
1. Use MMR to obtain the initial value of $\mathbf{G}$ under $\rho = 0$.
2. Given $\mathbf{G}$ and ρ from the last step, use Formula (8) to calculate $\hat{\boldsymbol{\beta}}$.

3. Given $\hat{\boldsymbol{\beta}}$ and $\mathbf{G}$ from the last step, use the combination method of golden section search and successive parabolic interpolation (Brent, 1973) to obtain ρ by maximizing Formula (7) or (10).
4. Given ρ and $\hat{\boldsymbol{\beta}}$ from the last step, use the Broyden–Fletcher–Goldfarb–Shanno (BFGS) algorithm (Fletcher, 1987) to obtain $\mathbf{G}$ by maximizing Formula (7) or (10).
5. Replicate steps 2–4 until convergency in terms of the maximum log-likelihood value in Formula (7) or (10).
6. Obtain the final estimations of $\boldsymbol{\beta}$, $\mathbf{G}$ and ρ and calculate the covariance of $\hat{\boldsymbol{\beta}}$ based on (9).
7. Estimate $\boldsymbol{\xi}_i$ using the approach presented in Section 2.4.

2.3. Hypothesis testing and model selection

The main parameters of interest in statistical inference may be the fixed effect parameter $\boldsymbol{\beta}$, the spatial autocorrelation parameter ρ, and the random effect parameters $\{\boldsymbol{\xi}_i\}$.

For $\boldsymbol{\beta}$, we used the multivariate Wald test (Harrell, 2015) to test the hypothesis with the null hypothesis (H_0) of $\boldsymbol{\beta} = \mathbf{0}$ and the alternative hypothesis (H_1) of $\boldsymbol{\beta} \neq \mathbf{0}$. The test statistic is

$$\text{Wald} = \hat{\boldsymbol{\beta}}^{\mathrm{T}} \text{cov}\left(\hat{\boldsymbol{\beta}}\right)^{-1} \hat{\boldsymbol{\beta}},$$

which follows an asymptotical chi-square (χ^2) distribution with degrees of freedom equal to the number of dimensions of $\boldsymbol{\beta}$. When a subset of elements in $\boldsymbol{\beta}$, for example, the coefficients of a specific covariate, are of interest, an extensive Wald test, with H_0 of $\mathbf{Z}\boldsymbol{\beta} = \mathbf{0}$ and H_1 of $\mathbf{Z}\boldsymbol{\beta} \neq \mathbf{0}$, can be used. $\mathbf{Z}$ is a matrix that makes $\mathbf{Z}\boldsymbol{\beta}$ the parameter of interest. The extensive test statistic is

$$\text{Wald} = \hat{\boldsymbol{\beta}}^{\mathrm{T}} \mathbf{Z}^{\mathrm{T}} \mathbf{Z} \text{cov}\left(\hat{\boldsymbol{\beta}}\right)^{-1} \mathbf{Z}^{\mathrm{T}} \mathbf{Z} \hat{\boldsymbol{\beta}}$$

which follows an asymptotical χ^2 distribution with degrees of freedom equal to the number of rows of $\mathbf{Z}$. In addition, for $\hat{\boldsymbol{\beta}}$ from the ML method, the general likelihood ratio (LR) test is also appropriate. However, for $\hat{\boldsymbol{\beta}}$ from the REML method, a modified LR test is needed (Roger, 1997; MGK and JHR, 2009).

For ρ, we used the LR test to test the hypothesis with H_0 of $\rho = 0$ and H_1 of $\rho \neq 0$. For the ML estimator, the test statistic is

$$\text{LR}_{\text{ML}} = -2\left[\sup_{\boldsymbol{\beta},\mathbf{V}} LL\left(\boldsymbol{\beta}, \mathbf{V}|\hat{\boldsymbol{\theta}}^*, \mathbf{X}^*, \mathbf{D}, \rho = 0\right) - \sup_{\boldsymbol{\beta},\mathbf{V},\rho} LL\left(\boldsymbol{\beta}, \mathbf{U}, \mathbf{V}|\hat{\boldsymbol{\theta}}^*, \mathbf{X}^*, \mathbf{D}\right)\right],$$

which follows an asymptotical χ^2 distribution with one degree of freedom. For the REML estimator, the LR test is also appropriate due to the identical fixed effects structures under H_0 and H_1, and the test statistic is

$$\text{LR}_{\text{REML}} = -2\left[\sup_{\boldsymbol{\beta},\mathbf{V}} RLL\left(\boldsymbol{\beta}, \mathbf{V}|\hat{\boldsymbol{\theta}}^*, \mathbf{X}^*, \mathbf{D}, \rho = 0\right) - \sup_{\boldsymbol{\beta},\mathbf{V},\rho} RLL\left(\boldsymbol{\beta}, \mathbf{U}, \mathbf{V}|\hat{\boldsymbol{\theta}}^*, \mathbf{X}^*, \mathbf{D}\right)\right].$$

For $\{\boldsymbol{\xi}_i\}$, we may focus on whether region-level random effects exist, i.e., whether the heterogeneity among regions exists after adjusting for the covariates. In this case, the interesting hypothesis is that H_0 of $\mathbf{U} \otimes \mathbf{V} = \mathbf{0}$ vs. H_1 of $\mathbf{U} \otimes \mathbf{V} \neq \mathbf{0}$. The multivariate extension of the Cochran Q test (Ritz et al., 2008), as in Gasparrini et al.'s work (Gasparrini et al., 2012), is also appropriate, and the detailed derivation can be seen in the supplementary material file via https://github.com/winkey1230/MCMAR. The test statistic is

$$Q = \sum_{i=1}^{m} (\hat{\boldsymbol{\theta}}_i - \mathbf{X}_i\hat{\boldsymbol{\beta}})^{\mathrm{T}} \mathbf{S}_i^{-1} (\hat{\boldsymbol{\theta}}_i - \mathbf{X}_i\hat{\boldsymbol{\beta}}),$$

where $\hat{\boldsymbol{\beta}}$ is the estimated fixed effect parameter from Eq. (8) without random effects, i.e., with $\boldsymbol{\Sigma} = \mathbf{D}$. Q follows an asymptotical χ^2 distribution with $(m-p)\,k$ degrees of freedom. In addition, the intensity of the region-level heterogeneity of the ERR can be calculated using the common H^2 and I^2 as follows:

$$H^2 = \max\{1, \frac{Q}{(m-p)\,k}\},$$
$$I^2 = \frac{H^2 - 1}{H^2},$$

where H^2 and I^2 measure the relative excess heterogeneity over that explained by sampling error and the proportion of region-level heterogeneity to total variation, respectively. Notably, the Cochran Q test in MCMAR is the same as that in MMR due to the identical models under the null hypothesis.

In practical studies, we may make a choice between MMR and MCMAR. The following two common recommendations may be available: (1) when the P value for the hypothesis test of $\rho = 0$ is smaller than the prespecified test level, such as 0.05, MCMAR is selected; otherwise, MMR is used; (2) the model with a smaller Akaike information criterion (AIC) or Bayesian information criterion (BIC) is selected.

2.4. Spatially smoothed average ERR and region-specific ERRs

Given a set of region-level predictors labeled $\boldsymbol{x}_0$, let

$$\mathbf{X}_0 = \mathbf{I}_k \otimes \boldsymbol{x}_0^T = \begin{bmatrix} \boldsymbol{x}_0^T & \mathbf{0} & \cdots & \mathbf{0} \\ \mathbf{0} & \boldsymbol{x}_0^T & & \mathbf{0} \\ \vdots & & \ddots & \vdots \\ \mathbf{0} & \mathbf{0} & \cdots & \boldsymbol{x}_0^T \end{bmatrix}.$$

The average ERR under $\boldsymbol{x}_0$ is defined by $\hat{\boldsymbol{\theta}}_0$ as follows:

$$\hat{\boldsymbol{\theta}}_0 = \mathbf{X}_0\hat{\boldsymbol{\beta}},$$
$$\mathrm{Cov}\left(\hat{\boldsymbol{\theta}}_0\right) = \mathbf{X}_0 \mathrm{cov}\left(\hat{\boldsymbol{\beta}}\right)\mathbf{X}_0^{\mathrm{T}}.$$

When the average ERR across all the studied regions is the focus, an MCMAR model including only the intercept is constructed, and the average ERR is defined by $\hat{\boldsymbol{\beta}}$ and $\mathrm{cov}\left(\hat{\boldsymbol{\beta}}\right)$.

The spatially smoothed region-specific ERRs are defined by $\{\hat{\boldsymbol{\theta}}_i^{'}\}$ as follows:

$$\hat{\boldsymbol{\theta}}_i^{'} = \mathbf{X}_i\hat{\boldsymbol{\beta}} + \hat{\boldsymbol{\xi}}_i,$$
$$\mathrm{cov}\left(\hat{\boldsymbol{\theta}}_i^{'}\right) = \mathbf{X}_i \mathrm{cov}\left(\hat{\boldsymbol{\beta}}\right)\mathbf{X}_i^{\mathrm{T}} + \mathrm{cov}\left(\hat{\boldsymbol{\xi}}_i\right),$$

where $\hat{\boldsymbol{\xi}}_i$ is the estimated region-level random effect in region i, i.e., the ith column vector in matrix $\hat{\boldsymbol{\xi}}$ (the estimation of $\boldsymbol{\xi}$). Let $\hat{\boldsymbol{\xi}}^* = \mathrm{vec}\left(\hat{\boldsymbol{\xi}}\right)$, and the best linear unbiased estimation (BLUE) of $\hat{\boldsymbol{\xi}}^*$ is (the detailed derivation can be seen in the supplementary materials):

$$\hat{\boldsymbol{\xi}}^* = \left(\hat{\mathbf{U}} \otimes \hat{\mathbf{V}}\right)\left(\hat{\mathbf{U}} \otimes \hat{\mathbf{V}} + \mathbf{D}\right)^{-1}\left(\hat{\boldsymbol{\theta}}^* - \mathbf{X}^*\hat{\boldsymbol{\beta}}\right),$$
$$\mathrm{cov}\left(\hat{\boldsymbol{\xi}}^*\right) = \left(\hat{\mathbf{U}} \otimes \hat{\mathbf{V}}\right) - \left(\hat{\mathbf{U}} \otimes \hat{\mathbf{V}}\right)\left(\hat{\mathbf{U}} \otimes \hat{\mathbf{V}} + \mathbf{D}\right)^{-1}\left(\hat{\mathbf{U}} \otimes \hat{\mathbf{V}}\right).$$

$\hat{\boldsymbol{\xi}}_i$ and $\mathrm{cov}\left(\hat{\boldsymbol{\xi}}_i\right)$ can be easily obtained by extracting the specific elements in $\hat{\boldsymbol{\xi}}^*$ and $\mathrm{cov}\left(\hat{\boldsymbol{\xi}}^*\right)$, respectively.

When we need to predict the ERR, defined by $\hat{\boldsymbol{\theta}}'_{new}$, in a new region, based on Expression (6), $\hat{\boldsymbol{\theta}}'_{new}$ can be calculated as

$$\hat{\boldsymbol{\theta}}'_{new} = \mathbf{X}_{new}\hat{\boldsymbol{\beta}} + \hat{\boldsymbol{\xi}}_{new} = \mathbf{X}_{new}\hat{\boldsymbol{\beta}} + \frac{\hat{\rho}}{1-\hat{\rho}+\hat{\rho}\mathcal{N}_{new}} \sum_{i\sim new} \hat{\boldsymbol{\xi}}_i, \tag{11}$$

where $\mathbf{X}_{new}$ is the predictor matrix in the new region. As such, MCMAR is able to obtain a high-resolution spatial distribution in ERRs.

3. Motivating example

In this section, a published motivating example was used to compare MCMAR to MMR. This example derives from Xiong et al.'s work (Xiao et al., 2017), in which the commonly used MMR-based two-stage strategy was employed to study the ERRs between temperature and hand, foot and mouth disease (HFMD) from 143 prefecture-level cities in China. In the first stage, a DLNM was independently constructed for each city to obtain a rough region-specific ERR. Then a multivariate meta-regression was used to obtain the average ERR and explore the causes of heterogeneity in ERRs. In this work, based on the region-specific ERRs estimated in the first stage by Xiong et al.'s work, we used the proposed MCMAR model to reanalyze the ERRs in the second stage. Then, the reanalyzed result was compared to that in Xiong et al.'s work. Notably, the spatial distribution of ERRs was not presented by Xiong et al. possibly due to the limitation of MMR.

3.1. ERR between temperature and HFMD

HFMD, caused by an enterovirus, has become a predominant childhood acute infectious disease in the Asia-Pacific region during the last two decades (Huang et al., 2018; Zhuang et al., 2015). Especially in mainland China, HFMD has caused a heavy disease burden, with the highest disability-adjusted life-years in children and more than one million cases reported annually (Koh et al., 2018; Xing et al., 2014). It is well known that temperature is one of the most important environmental factors related to HFMD, affecting the transmission of the disease by impacting virus reproduction, survival, and children's behaviors (Belanger et al., 2009; Bertr et al., 2012; Yi et al., 2019; Cheng et al., 2018). Various studies (Yi et al., 2019; Cheng et al., 2018; Zhu et al., 2016; Nguyen et al., 2017) have shown that the relationship between temperature and HFMD may differ across regions due to the heterogeneity of the natural environment and economic development levels. Studying the spatial distribution of heterogeneous ERRs and the causes of heterogeneity will help to deepen the understanding of the temperature-HFMD ERR, to identify highly sensitive regions and to design region-specific public health interventions, which play important roles in HFMD control and prevention.

3.2. Data

In Xiong et al.'s well-presented work, the daily clinical cases of HFMD among children aged 0–12 years for each of 143 prefecture-level cities of mainland China between 2009 and 2014 were recorded. Data for a total of 3,060,450 cases were collected. The daily relative mean temperature was used as the studied environmental factor. In addition, the daily relative humidity, air pressure, rainfall and sunshine hours were also collected as potential confounders in the ERR between temperature and HFMD. The detailed descriptive analysis can be found in Xiong et al.'s work.

3.3. The first stage: Modeling city-specific ERRs

In the first stage, Xiong et al. used a DLNM to characterize the nonlinear exposure–response and lag–response relationship between daily mean temperature and daily HFMD cases for each city. To ensure DLNMs for all cities to yield non-missing estimates, the mean temperatures were scaled

based on city-specific percentiles. A quasi-Poisson distribution with overdispersion was selected. For each city, the DLNM was expressed as

$$Y_t \sim \text{Quasi} - \text{Poisson}\left(\mu_{it}\right),$$
$$\ln\left(\mu_t\right) = \alpha + cb\left(Tem; \boldsymbol{\eta}\right) + Confounders + Autoterms,$$

where Y_t is the observed number of HFMD cases at time t in the specific city. *Confounders* indicates the confounding effects from daily relative humidity, air pressure, rainfall, sunshine hours, holidays, weekends, long-term trends, and seasonality. *Autoterms* are the autoregressive terms of HFMD daily counts on the logarithm scale at lag 1 and 2, which were selected based on the autocorrelation plot of residuals. $cb\left(Tem; \boldsymbol{\eta}\right)$ is the cross-basis function regarding the relative mean temperatures, with a lag range of 4–14 days, 5-degrees of freedom (df) natural cubic splines for the exposure–response dimension and 4-df natural cubic splines for the lag–response dimension, where $\boldsymbol{\eta}$ is the parameter to be estimated and dfs are selected based on the quasi-AIC. More specifically, let $\boldsymbol{x}_t = \left[Tem_{t-4}, Tem_{t-5}, \ldots, Tem_{t-14}\right]^{\mathrm{T}}$ and $\updownarrow = [4, 5, 6, \ldots, 14]^{\mathrm{T}}$, then $cb\left(Tem; \boldsymbol{\eta}\right)$ can be written as

$$cb\left(Tem; \boldsymbol{\eta}\right) = cb\left(\boldsymbol{x}_t; \boldsymbol{\eta}\right) = \sum_{k=1}^{5}\sum_{j=1}^{4} \boldsymbol{q}_{k\cdot}^{(t)} \boldsymbol{c}_{\cdot j}\eta_{kj} = \mathbf{w}^{(\boldsymbol{t})}\boldsymbol{\eta}$$

where $\boldsymbol{q}_{k\cdot}^{(t)}$ is the kth row of 5×11 basis matrix $\mathbf{q}^{(t)}$ obtained by the application of the natural-cubic-spline basis functions to the original $\boldsymbol{x}_t$. $\boldsymbol{c}_{\cdot j}$ is the jth column of 11×4 basis matrix $\mathbf{c}$ obtained by the application of the natural-cubic-spline basis functions to $\updownarrow$. $\boldsymbol{\eta}$ is an unknown 20-dimensional vector composed of $\{\eta_{kj}\}$. The maximum likelihood method is used to estimate the value of $\boldsymbol{\eta}$. Let $\mathbf{M} = \boldsymbol{l}_{11}^{\mathrm{T}}\mathbf{c} \bigotimes \mathbf{I}_5$ where $\boldsymbol{l}_{11}^{\mathrm{T}}$ is a 11-dimensional vector of one, then, the accumulative temperature-HFMD ERR for city i is defined by a 5-dimensional vector $\boldsymbol{\theta}_i$, estimated as

$$\hat{\boldsymbol{\theta}}_i = \mathbf{M}\hat{\boldsymbol{\eta}}_i,$$
$$\text{Cov}\left(\hat{\boldsymbol{\theta}}_i\right) = \mathbf{M}\text{cov}\left(\hat{\boldsymbol{\eta}}_i\right)\mathbf{M}^{\mathrm{T}}.$$

The detailed methodology of defining ERR in DLNM can be found in Gasparrini et al.'s works (Gasparrini, 2014; Gasparrini and Armstrong, 2013).

3.4. The second stage: Mapping the ERRs and identifying the causes of heterogeneity

In the second stage, Xiong et al. used MMR with only the intercept to obtain the average ERR across 143 cities and used MMR with a single region-level predictor to study the heterogeneity attributable to the predictor. In this work, we further used MCMAR to achieve the same objectives and compared the results to those from MMR. The spatially adjacent relationships among cities were constructed based on an empirical 4-nearest neighbors method. The other methods, such as 3, 5, 6-nearest neighbors methods and the Thiessen-polygons-based method, were also selected as sensitivity analyses. The details are shown in the supplementary material.

The comparison of heterogeneity is shown in Table 1. The Cochran Q test showed significant region-level heterogeneity in ERRs. Using the LR test, MMR identified eight of sixteen predictors that significantly contributed to the heterogeneity ($P < 0.05$), while MCMAR identified no predictor ($P > 0.05$). In all the models, MCMAR achieved considerably smaller AICs than MMR, which suggests that MCMAR may obtain more accurate results than MMR. Statistical tests for $\rho = 0$ in MCMAR showed that the spatial autocorrelation of ERRs significantly existed in all the models ($P < 0.001$), suggesting the reasonableness of incorporating spatial autocorrelation into the second-stage model. In addition, we also constructed MMR or MCMAR with multiple predictors, which were selected using a forward method based on AIC. In MCMAR, no predictor was deserved to be incorporated. In MMR, four predictors, i.e., average rainfall, longitude, GDP increase, and average temperature, were incorporated, and the first three were identified as the significant causes contributing to the heterogeneity ($P < 0.001$) and the average temperature was not identified ($P = 0.06$). Furtherly, the AIC of MMR with the four predictors was still considerably larger than that of MCMAR with only intercept (497.6 vs 469.7).

Table 1
Comparison between MMR and MCMAR in terms of investigating the heterogeneity attributable to region-level predictors.

Model including a single predictor	AIC		Test predictor (P)		ρ in MCMAR[a]		Cochran Q test[b]	
	MMR	MCMAR	MMR	MCMAR	ρ value	P	I^2	P
Intercept only[c]	527.9	469.7	NA	NA	0.531	<0.001	68.5	<0.001
Latitude	514.8	472.8	<0.001	0.229	0.452	<0.001	67	<0.001
Longitude	527	475.9	0.053	0.576	0.501	<0.001	68.2	<0.001
Altitude	522.4	471.5	0.008	0.143	0.497	<0.001	67.7	<0.001
Temperature	514.3	470.5	<0.001	0.1	0.461	<0.001	66.9	<0.001
Relative humidity	515.1	474.8	<0.001	0.428	0.463	<0.001	67.1	<0.001
Air pressure	521.6	471.1	0.006	0.124	0.496	<0.001	67.6	<0.001
Rainfall	501.3	471.6	<0.001	0.152	0.385	<0.001	66.5	<0.001
Sunshine hours	523.2	472.8	0.011	0.231	0.501	<0.001	67.6	<0.001
Population increase	536.4	476.8	0.905	0.714	0.543	<0.001	68.5	<0.001
Population density	531.5	471.5	0.265	0.147	0.569	<0.001	68.6	<0.001
GDP per person	529	472.4	0.11	0.201	0.525	<0.001	68.3	<0.001
GDP increase	527.4	469.6	0.061	0.072	0.543	<0.001	68.4	<0.001
Licensed physicians	535.1	478.7	0.719	0.96	0.527	<0.001	68.6	<0.001
Hospital beds	535.5	476	0.785	0.601	0.544	<0.001	68.6	<0.001
Travel passengers	532.5	473.3	0.37	0.269	0.542	<0.001	68.6	<0.001
Number of students	535	476.5	0.718	0.666	0.536	<0.001	68.2	<0.001

Note: The parameters in MMR and MCMAR were estimated using the ML method, and the REML method gave a similar result, which can be found in the supplementary material.
[a]The LR test was used to test the spatial autocorrelation in MCMAR.
[b]The Cochran Q test presents the same results for MMR and MCMAR due to the identical model under the null hypothesis.
[c]"Intercept only" indicates the MMR without any region-level predictor, so the test results for predictors are not available (NA).

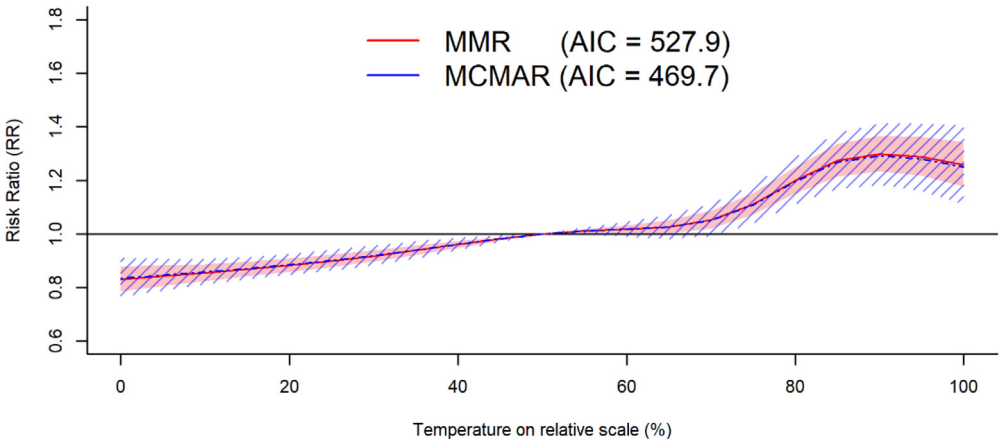

Fig. 1. The pooled average ERR curves obtained by MMR and MCMAR with only intercepts.

The comparison of the pooled average ERRs across all cities obtained by MMR and MCMAR, both with only intercepts, is shown in Fig. 1. As in Xiong et al.'s work, intuitive ERR curves with a 50% quantile of temperature as a reference were presented. The results showed that MMR and MCMAR obtained highly similar average ERRs, while the 95% confidence interval in MCMAR was wider than that in MMR, which conformed to our expectation because MMR would underestimate the variation due to ignoring the between-region correlation of ERRs.

We also compared the spatial distributions of ERRs estimated by MMR and MCMAR. For a more intuitive exhibition, we used MMR and MCMAR with only intercepts to calculate the pooled relative risks (RRs) at 10%, 30%, 70% and 90% quantiles of temperature referring to 50% for each

Table 2
The parameter settings for the eight simulation scenarios.

Scenarios	Parameter for intercept ($\boldsymbol{\beta}_0$)	Parameter for predictor ($\boldsymbol{\beta}_1$)	ρ
Scen1-rho0	(0.169, 0.132, 0.107, 0.237, 0.072)	(0.002, 0.002, 0.013, 0.010, 0.011)	0
Scen1-rho1	(0.169, 0.132, 0.107, 0.237, 0.072)	(0.002, 0.002, 0.013, 0.010, 0.011)	0.3
Scen1-rho2	(0.169, 0.132, 0.107, 0.237, 0.072)	(0.002, 0.002, 0.013, 0.010, 0.011)	0.5
Scen1-rho3	(0.169, 0.132, 0.107, 0.237, 0.072)	(0.002, 0.002, 0.013, 0.010, 0.011)	0.8
Scen2-rho0	(0.198, 0.145, 0.219, 0.33, 0.138)	(0, 0, 0, 0, 0)	0
Scen2-rho1	(0.198, 0.145, 0.219, 0.33, 0.138)	(0, 0, 0, 0, 0)	0.3
Scen2-rho2	(0.198, 0.145, 0.219, 0.33, 0.138)	(0, 0, 0, 0, 0)	0.5
Scen2-rho3	(0.198, 0.145, 0.219, 0.33, 0.138)	(0, 0, 0, 0, 0)	0.8

Note: For the first four scenarios, $\boldsymbol{\beta}_0$ and $\boldsymbol{\beta}_1$ are the estimated fixed effects in MMR with rainfall as a predictor in the motivating example. For the last scenarios, $\boldsymbol{\beta}_0$ is the estimated intercept in MCMAR with only the intercept.

city. The comparison of spatial distributions is shown in Fig. 2. MCMAR achieved a smoother spatial distribution than MMR, which was considerably found in RRs at the 90% quantile of temperature. The representative regions for comparison are marked by blue circles or ellipses, with that the RRs obtained by MMR show steeper distinction between adjacent cities than those obtained by MCMAR. The spatial distributions of ERRs show that high temperature increases the risk of HFMD mainly in the South and Northeast of China, but which does not in the Central.

4. Simulation study

The comparison between MMR and MCMAR in the motivating example may be somewhat subjective, especially for the comparison regarding spatial distributions, i.e., the city-specific predictions of ERRs. Therefore, we generated a batch of simulation datasets to further provide an objective comparison.

4.1. Simulation scenario setting and data generation process

Two situations were considered. One (Scen1) is that an observed predictor is able to explain part of the region-level heterogeneity, as shown in MMR, and the other (Scen2) is that there is no observed predictor able to explain the heterogeneity, as shown in MCMAR. For the former, rainfall was selected as the observed predictor as in Xiong et al.'s work, and the true parameters, i.e., the intercept ($\boldsymbol{\beta}_0$) and regression coefficient ($\boldsymbol{\beta}_1$) for the predictor, were set as the estimations from MMR with rainfall in the motivating example. For the latter, the intercept was set as the estimation from MCMAR with only the intercept, and $\boldsymbol{\beta}_1$ was set as $\mathbf{0}$. For each situation, four different values were set to simulate different intensities of spatial autocorrelation in practical studies, i.e., $\rho = 0, 0.3, 0.5, 0.8$. Other necessary parameters, including $\{\mathbf{S}_i\}$, $\mathbf{V}$ and $\mathbf{U}$, also came from the motivating example. As such, a total of 8 simulation scenarios were set, which are shown in Table 2. For each scenario, the true ERR, $\boldsymbol{\theta}_i$, for city i is

$$\boldsymbol{\theta}_i = \boldsymbol{\beta}_0 + x_i\boldsymbol{\beta}_1 + \boldsymbol{\xi}_i$$

where x_i is the predictor. $\boldsymbol{\xi}_i$ is the ith column of matrix $\boldsymbol{\xi}$, which is sampled from the matrix normal distribution with known $\mathbf{V}$ and $\mathbf{U}$, as shown in Formula (3). Finally, we repeated the following random sampling 1000 times to simulate the estimated city-specific ERRs in the first stage.

$$\hat{\boldsymbol{\theta}}_i \sim MN\left(\boldsymbol{\theta}_i, \mathbf{S}_i\right).$$

The true parameters and the simulated random datasets are available at the appendices.

4.2. Parameter estimations and performance measures

For each simulation dataset, MMR and MCMAR with only intercepts were used to obtain the average ERR, i.e., to estimate $\boldsymbol{\beta}_0$. MMR and MCMAR with a predictor were used to investigate

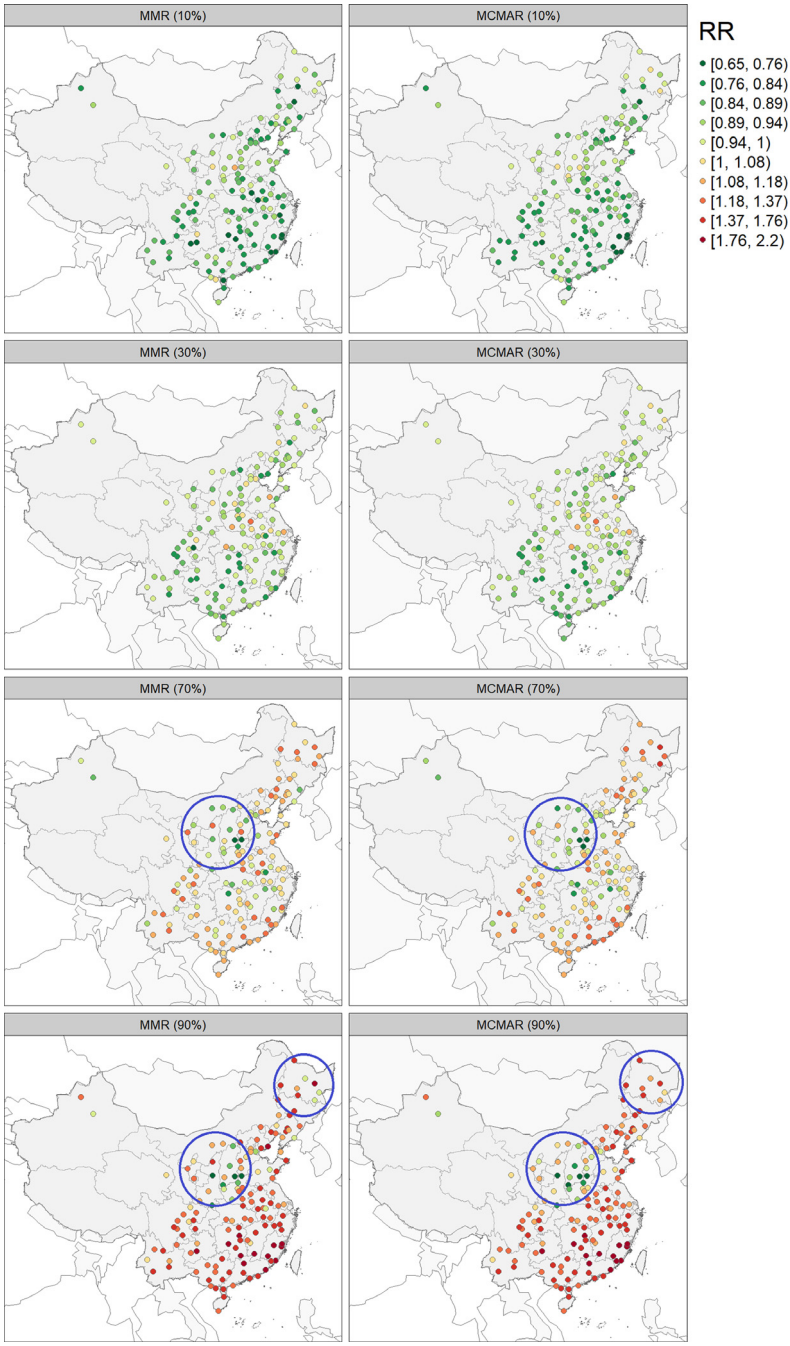

Fig. 2. The comparison of spatial distributions of ERRs estimated by MMR and MCMAR in terms of RR at the 10%, 30%, 70% and 90% quantiles of temperature referring to 50%.

whether the incorporated predictor contributed to the region-level heterogeneity, i.e., to estimate $\boldsymbol{\beta}_1$ and test the hypothesis of $\boldsymbol{\beta}_1 = \mathbf{0}$. For all the models, the pooled city-specific ERRs, i.e., $\boldsymbol{\theta}_i$, were estimated to reflect the spatial distribution, and the AIC values were calculated to evaluate the fit performance. In addition, for both model strategies, i.e., with only intercept and with a predictor, the optimal model (OPT) was selected from MMR and MCMAR based on the hypothesis test of $\rho = 0$. Specifically, when $P < 0.05$, MCMAR was chosen, and MMR was used otherwise. As such, a total of six model results were obtained for each dataset.

For each model in a dataset, the relative vector distance from the estimated parameter to the true parameter was used to measure the estimated error if the true parameter vector included no element of zero; otherwise, the absolute vector distance was used. Specifically, for $\boldsymbol{\beta}_0$, the relative distance was used. For $\boldsymbol{\beta}_1$, the relative and absolute distances were used in Scen1 and Scen2, respectively. For $\boldsymbol{\theta}_i$, the absolute distance was used due to zero-closed elements existing. Then, we averaged the absolute or relative vector distances over replicas to obtain the mean absolute error (MAE) or relative mean absolute error (RMAE) for each model in each scenario. The MAE and RMAE can be calculated as

$$\mathrm{RMAE}_{\boldsymbol{\beta}_0} = \frac{1}{1000}\sum_{s=1}^{1000}\left\|\frac{\hat{\boldsymbol{\beta}}_0^{(s)} - \boldsymbol{\beta}_0}{\boldsymbol{\beta}_0}\right\|, \mathrm{RMAE}_{\boldsymbol{\beta}_1\neq\mathbf{0}} = \frac{1}{1000}\sum_{s=1}^{1000}\left\|\frac{\hat{\boldsymbol{\beta}}_1^{(s)} - \boldsymbol{\beta}_1}{\boldsymbol{\beta}_1}\right\|,$$

$$\mathrm{MAE}_{\boldsymbol{\beta}_1=\mathbf{0}} = \frac{1}{1000}\sum_{s=1}^{1000}\left\|\hat{\boldsymbol{\beta}}_1^{(s)} - \boldsymbol{\beta}_1\right\|, \mathrm{MAE}_{\boldsymbol{\theta}_i} = \frac{1}{1000}\sum_{s=1}^{1000}\frac{1}{143}\sum_{i=1}^{143}\left\|\hat{\boldsymbol{\theta}}_i'^{(s)} - \boldsymbol{\theta}_i\right\|.$$

The average AIC, the power of identifying $\boldsymbol{\beta}_1 \neq \mathbf{0}$ in Scen1, and the false positive error (FPE) of identifying $\boldsymbol{\beta}_1 \neq \mathbf{0}$ in Scen2 were calculated as

$$\text{Average AIC} = \frac{1}{1000}\sum_{s=1}^{1000}\mathrm{AIC}_i,$$

$$\mathrm{Power}_{\mathrm{Scen1}} = \frac{1}{1000}\sum_{s=1}^{1000}I(P_{\boldsymbol{\beta}_1} < 0.05), \mathrm{FPE}_{\mathrm{Scen2}} = \frac{1}{1000}\sum_{s=1}^{1000}I(P_{\boldsymbol{\beta}_1} < 0.05).$$

In addition, the coverage rates of 95% confidence intervals for $\boldsymbol{\beta}_0$ and $\boldsymbol{\beta}_1$ are also calculated to compare the uncertainty between MMR and MCMAR. Because $\boldsymbol{\beta}_0$ and $\boldsymbol{\beta}_1$ are vectors and the 95% confidence intervals are high-dimensional and not intuitive, we use the multivariate Wald test to judge whether the 95% confidence interval covers the true parameter. Taking $\boldsymbol{\beta}_1$ as an example, the test statistic can be constructed as

$$\mathrm{Wald} = \left(\hat{\boldsymbol{\beta}}_1 - \boldsymbol{\beta}_1\right)^{\mathrm{T}}\mathrm{cov}\left(\hat{\boldsymbol{\beta}}_1\right)^{-1}\left(\hat{\boldsymbol{\beta}}_1 - \boldsymbol{\beta}_1\right)$$

which follows an asymptotical χ^2 distribution with degrees of freedom equal to the number of dimensions of $\boldsymbol{\beta}_1$. When the P value of the test statistic is larger than 0.05, the 95% confidence interval covers the true parameter $\boldsymbol{\beta}_1$, otherwise it does not cover. The coverage rate is more closed to 0.95, and the performance for uncertainty is better.

4.3. Results

The comparison of the simulation results between MMR and MCMAR is shown in Table 3. As expected, MMR performed best in scenarios with no spatial autocorrelation, i.e., Scen1-rho0 and Scen2-rho0, whereas MCMAR performed very similarly to MMR and even obtained a smaller RMAE for $\boldsymbol{\beta}_0$, as seen in Scen1-rho0. In scenarios with $\rho \neq 0$, MCMAR outperformed MMR considerably in estimating the average and city-specific ERRs, estimating the effect of predictors, identifying the causes of heterogeneity, and evaluating the model fit based on the AIC. Overall, the advantage increased as ρ increased. In Scen2 without any observed predictor contributing to the region-level heterogeneity of ERRs, MMR with a predictor had a high rate of falsely identifying the predictor as

Table 3
Comparison between MMR and MCMAR in the simulation study.

Scenarios	Model with only intercept			Model with a predictor		
	MMR	MCMAR	OPT[a]	MMR	MCMAR	OPT
RMAE for β_0[b]; RMAE for β_1 in Scen1; MAE for β_1 in Scen2						
Scen1-rho0	0.253	0.25	0.252	1.228	1.235	1.23
Scen1-rho1	0.241	0.225	0.225	1.577	1.363	1.364
Scen1-rho2	0.481	0.432	0.432	2.503	2.4	2.4
Scen1-rho3	0.359	0.326	0.326	3.45	2.823	2.823
Scen2-rho0	0.379	0.379	0.379	0.006	0.006	0.006
Scen2-rho1	0.358	0.348	0.348	0.006	0.006	0.006
Scen2-rho2	0.69	0.661	0.661	0.008	0.008	0.008
Scen2-rho3	0.649	0.615	0.615	0.014	0.01	0.01
Coverage rates of 95% confidence intervals for β_0 in model with only intercept and for β_1 in model with a predictor						
Scen1-rho0	0.954	0.971	0.957	0.981	0.976	0.981
Scen1-rho1	0.914	0.995	0.995	0.883	0.972	0.972
Scen1-rho2	0.422	0.977	0.977	0.547	0.853	0.853
Scen1-rho3	0.027	0.751	0.751	0.027	0.571	0.571
Scen2-rho0	0.977	0.971	0.976	0.984	0.98	0.982
Scen2-rho1	0.926	0.992	0.992	0.868	0.962	0.962
Scen2-rho2	0.486	0.95	0.95	0.501	0.843	0.843
Scen2-rho3	0.003	0.437	0.437	0.029	0.569	0.569
MAE for city-specific ERRs						
Scen1-rho0	0.468	0.469	0.468	0.466	0.467	0.466
Scen1-rho1	0.397	0.384	0.384	0.394	0.382	0.382
Scen1-rho2	0.386	0.366	0.366	0.381	0.363	0.363
Scen1-rho3	0.371	0.334	0.334	0.344	0.329	0.329
Scen2-rho0	0.463	0.464	0.464	0.466	0.467	0.466
Scen2-rho1	0.389	0.38	0.38	0.395	0.384	0.384
Scen2-rho2	0.379	0.361	0.361	0.381	0.363	0.363
Scen2-rho3	0.349	0.326	0.326	0.343	0.328	0.328
Average AIC values over the replicas[c]						
Scen1-rho0	424.236	424.59	423.815	452.762	453.894	452.676
Scen1-rho1	246.129	202.118	202.118	256.6	238.924	238.925
Scen1-rho2	182.777	131.715	131.715	189.74	160.916	160.916
Scen1-rho3	196.18	92.058	92.058	166.178	122.547	122.547
Scen2-rho0	395.242	396.455	395.15	454.459	455.701	454.38
Scen2-rho1	196.251	179.056	179.06	254.89	237.473	237.477
Scen2-rho2	133.552	102.601	102.601	188.474	159.374	159.374
Scen2-rho3	122.048	67.868	67.868	165.806	121.962	121.962
Power or false positive error of identifying the predictor contributing to heterogeneity						
Scen1-rho0	–	–	–	1	1	1
Scen1-rho1	–	–	–	1	1	1
Scen1-rho2	–	–	–	1	1	1
Scen1-rho3	–	–	–	1	1	1
Scen2-rho0	–	–	–	0.016	0.020	0.018
Scen2-rho1	–	–	–	0.132	0.038	0.038
Scen2-rho2	–	–	–	0.499	0.157	0.157
Scen2-rho3	–	–	–	0.971	0.431	0.431

Note: The parameters were estimated using the REML method. The comparison results based on the ML method can be found in the supplementary materials.

[a] OPT is the model selected from MMR and MCMAR based on the hypothesis test of $\rho = 0$.

[b] $\boldsymbol{\beta}_0$ defines the true average association across all regions.

[c] The values of AIC are calculated based on the penalized likelihood, so the comparison of AICs is only available between MMR and MCMAR with identical fixed effects structures.

being able to explain the heterogeneity, and the false positive rate increased as ρ was larger, even up to 0.971 when $\rho = 0.8$, which is unacceptable in practical studies. However, MCMAR with the predictor considerably reduced the false positive rate. In Scen1 with a predictor contributing to the region-level heterogeneity, both MMR and MCMAR achieved a power of 1 in correctly identifying

the predictor. The OPT model achieved performance closer to the ideal MMR in scenarios with $\rho = 0$ than MCMAR and did not reduce the advantage of MCMAR over MMR in scenarios with $\rho \neq 0$. For the coverage rates of 95% confidence intervals, in Scenario with no spatial dependence, both MMR and MCMAR obtained coverage rates closed to 0.95, while in scenarios with spatial dependence, the coverage rates obtained by MMR is much smaller than 0.95, especially in those with ρ = 0.3 or 0.8, by contrast, MCMAR obtained much better coverage rates.

5. Discussion

In this work, we combined LCAR with MMR to construct an extended model called MCMAR which can sufficiently utilize the spatial autocorrelation information between regions. Then, a novel MCMAR-based two-stage strategy was developed to map the ERRs between environment risk factors and health-related outcomes and identify the causes of heterogeneity. A motivating example and a simulation study demonstrated that, the MCMAR-based strategy exhibited considerably better performance than the classic MMR-based strategy. More accurate spatial distribution of ERRs and causes of heterogeneity are essential to make region-specific environment-related invention policies for promoting health, for example, decreasing the exposure to certain environment factor is more cost-effective in the regions with high-sensitivity risk. More notably, possibly due to the MMR-based strategy not considering the spatial distribution, the spatial distribution of short-term ERRs is less frequently focused on.

In the motivating example, the spatial distribution of temperature-HFMD ERRs shows that high temperature increases the risk of HFMD mainly in the South of China, but which does not in the Central, which suggests that high-temperature-related interventions for controlling HFMD should be carried out in the South rather than the Central. Compared to the MMR-based strategy, MCMAR achieved a considerably smaller AIC (469.7 vs. 527.9). The LR test regarding spatial autocorrelation, i.e., $\rho \neq 0$, also supported that a significant spatial autocorrelation existed in ERRs ($P < 0.001$). These results suggest that MCMAR may obtain more accurate results than the classic MMR. Regarding the identification of predictors contributing to city-level heterogeneity, MCMAR identified no observed predictor as significant, while MMR identified half of the observed predictors as significant. We further analyzed the spatial autocorrelation in the identified predictors. Moran's I test showed that significant spatial autocorrelations existed in these predictors, which suggests that the effect of predictors in MMR may be severely confounded by spatial autocorrelation. More specifically, if an observed false predictor (“false” denotes that the predictor does not contribute to the heterogeneity, and “true” denotes the opposite) and a batch of unobserved true predictors exhibited similar spatial autocorrelation patterns, MMR would attribute the effect of unobserved true predictors to the incorporated false predictor and thus lead to a false identification, while MCMAR would considerably relieve the confounding by adjusting spatial autocorrelation, which was also supported by the simulation study. Therefore, the identified predictors, e.g., rainfall, by MMR in Xiong et al.'s work may make a false positive error, at least, there is no enough evidence showing that these predictors contributed to the heterogeneity in the study. A false cause may mislead the policy and the understanding about the mechanism underlying the environment factors and health outcomes.

Comparing the average ERRs across all cities, MMR and MCMAR obtained similar point estimations, but MMR obtained a narrower confidence interval than MCMAR, which is explained by a statistical knowledge that ignoring the correlation among sample data will underestimate the variance, thus leading to an over-narrow confidence interval. Underestimated variance will reduce the accuracy of estimation in MMR. The simulation study also confirmed that MMR achieved worse performance than MCMAR in estimating the average and city-specific ERRs.

When predicting the ERR in a new location, which is necessary for characterizing high-resolution spatial distribution in the whole studied area, MMR is only able to utilize the fixed effect, e.g., $\hat{\boldsymbol{\theta}}'_{new} = \hat{\boldsymbol{\beta}}_0 + x_i\hat{\boldsymbol{\beta}}_1$, as in Wu and Zhao et al.'s works (Wu et al., 2022; Zhao et al., 2021). Especially when no predictor is included, the predictions for all new locations are identical, i.e., $\hat{\boldsymbol{\beta}}_0$ regardless of their spatial positions, which may lead to an unsatisfactory spatial distribution in ERRs. MCMAR is able to use both the spatial random effects and fixed effects to obtain the prediction as in Eq. (11), which provides a smoother and more rational spatial distribution. Therefore, in Wu and Zhao et al.'s

works, if MCMAR were used, a more accurate ERR spatial distribution might be obtained, and then the related attributable disease burdens would be evaluated more accurately, which are essential to make cost-effective region-specific policies for decreasing exposure and allocating medical sources. In addition, the MMR-based two-stage strategy has also been used to investigate the associations between meteorological factors and air pollutants, as in Yang et al.'s study (Yang et al., 2021), which is important for air pollutant control and forecast, so our strategy may provide a more accurate alternative tool in this field.

In the motivating example, the spatially adjacent relationships among cities were constructed based on the 4-nearest neighbors method, which may be somewhat arbitrary. We also used the 3-, 5- and 6-nearest neighbors methods and Thiessen polygon-based method to construct the spatially adjacent relationships as sensitivity analyses. MCMAR still outperformed MMR and the details can be found in the supplementary materials. Currently, many related studies have been carried out across the globe; in these cases, spatially adjacent relationships may be independently constructed for each continent due to their isolated spatial positions. In practical studies, model fit statistics, such as the AIC and BIC, can be used to select an appropriate method of constructing spatially adjacent relationships. In addition, the spatial locations of the studied regions may be sparsely distributed in practical studies, and the spatial autocorrelation of the ERR may be slight or may not even exist. In these cases, we can use the LR test to test whether the spatial autocorrelation, i.e., $\rho \neq 0$, actually exists and is significant; if significantly exists, MCMAR should be selected, and MMR should be selected otherwise. This selection may limit the overfitting risk derived from introducing false spatial autocorrelation, which is also supported by the simulation study regarding the performance of the OPT model. As model selection indicators, the AIC and BIC may also be appropriate for selecting either MCMAR or MMR.

In this study, an unstructured matrix was selected for $\mathbf{V}$ to maintain flexibility. However, in some cases, the dimension of the ERR-defining vector may be relatively large, and selecting an unstructured $\mathbf{V}$ will lead to many parameters to be estimated, which will result in unstable estimations and intensive use of computing resources. In these cases, selecting a structured $\mathbf{V}$ may be more appropriate, as in MMR. Without any prior, since both $\mathbf{V}$ and $\{\mathbf{S}_i\}$ reflect the correlations between elements in the ERR-defining vector, a structured $\mathbf{V}$ may be set by limiting the correlation reflected by $\mathbf{V}$ being same with the average correlation reflected by all the $\mathbf{S}_i$s.

Similar to MMR, MCMAR does not depend on raw data and only depends on result data from the first stage. Therefore, MCMAR can also be applied to published (or second-hand) datasets with spatial positions, including but not limited to ERR datasets, longitudinal profiles (Ishak et al., 2007), receiver operating characteristic (ROC) curves (Arends et al., 2008) and survival curves (Dear, 1994; Lidia et al., 2008). With the improvement in geographic information systems and disease surveillance systems, a large number of such spatial datasets have been and are being produced, which will provide MCMAR with a wide range of applications. Another issue worth noting is that if the ERR-defining vectors, estimated by a GAM, come from different studies, they cannot usually be used directly in MCMAR due to dimensional differences among vectors; even with an identical number of dimensions, the vectors also have different mathematical meanings due to different choices of spline functions. In such cases, the estimated relative risks with covariance can alternatively be used in MCMAR. Taking the ERR between temperature and HFMD as an example, first, a series of representative objective temperatures are selected. Then, for each region, the estimated ERR-defining vector from a GAM in the first stage is used to obtain the logarithmic relative risks vector with covariance over the reference temperature. Finally, the region-specific logarithmic relative risks vector with covariance can be used in MCMAR due to the similar epidemiological meanings. In this case, a structured $\mathbf{V}$ needs to be selected due to the large dimensions.

CRediT authorship contribution statement

Wei Wang: Conceptualized this study, Wrote the main manuscript text, Derived the methodology, Carried out the simulation, Case study. **Fang Liao:** Carried out the case study, Edited the manuscript. **Fei Yin:** Reviewed and edited the manuscript, Obtained the funding. **Yue Ma:** Conceptualized this study, Wrote the main manuscript text, Obtained the funding.

Declaration of competing interest

The authors declare that they have no known competing financial interests or personal relationships that could have appeared to influence the work reported in this paper.

Appendix

The supplementary materials include information on the methods of constructing spatially adjacent matrices, the sensitivity analysis results with different spatially adjacent matrices, and some formula derivations mentioned in the main text. The supplementary materials and the data and R codes for replicating our results are available from https://github.com/winkey1230/MCMAR.

References

Anselin, L., 1988. Spatial econometrics: methods and models.
Arends, L.R., Hamza, T.H., Houwelingen, J., Heijenbrok-Kal, M.H., Stijnen, T., 2008. Bivariate random effects meta-analysis of ROC curves. Med. Decis. Mak. 28 (5), 621–638.
Belanger, M., Gray-Donald, K., O'Loughlin, J., Paradis, G., Hanley, J., 2009. Influence of weather conditions and season on physical activity in adolescents. Ann. Epidemiol. 19 (3), 180–186.
Bertr, I., Schijven, J.F., Sanchez, G., et al., 2012. The impact of temperature on the inactivation of enteric viruses in food and water: a review. J. Appl. Microbiol. 112 (6), 1059–1074.
Besag, J., York, J., Mollié, A., 1991. Bayesian image restoration, with two applications in spatial statistics. Ann. Inst. Statist. Math. 43 (1), 1–20.
Brent, R.P., 1973. Algorithms for minimization without derivatives. Math. Comput. 19 (5).
Cheng, Q., Bai, L.J., Zhang, Y.W., et al., 2018. Ambient temperature, humidity and hand, foot, and mouth disease: A systematic review and meta-analysis. Sci. Total Environ. 625, 828–836.
Dear, K., 1994. Iterative generalized least squares for meta-analysis of survival data at multiple times. Biometrics 50 (4), 989–1002.
Fletcher, R., 1987. Practical Methods of Optimization, second ed..
Gasparrini, A., 2014. Modeling exposure-lag-response associations with distributed lag non-linear models. Stat. Med. 33 (5), 881–899.
Gasparrini, A., Armstrong, B., 2013. Reducing and meta-analysing estimates from distributed lag non-linear models. BMC Med. Res. Methodol. 13 (1), 1–10.
Gasparrini, A., Armstrong, B., Kenward, M.G., 2010. Distributed lag non-linear models. Stat. Med. 29 (21), 2224–2234.
Gasparrini, A., Armstrong, B., Kenward, M.G., 2012. Multivariate meta-analysis for non-linear and other multi-parameter associations. Stat. Med. 31 (29), 3821–3839.
Harrell, F.E., 2015. Regression modeling strategies: with applications to linear models, logistic and ordinal regression, and survival analysis.
Hedges, L.V., Olkin, I., 1985. Statistical methods for meta-analysis. In: New Directions for Program Evaluation. (24), pp. 25–42, 1984.
Huang, J., Liao, Q.H., Ooi, M.H., et al., 2018. Epidemiology of recurrent hand, foot and mouth disease, China, 2008–2015. Emerg. Infect. Diseases 24 (3), 432–442.
Ishak, K.J., Platt, R.W., Joseph, L., Hanley, J.A., Caro, J.J., 2007. Meta-analysis of longitudinal studies. Clin. Trials 4 (5), 525.
Katsouyanni, K., Touloumi, G., Spix, C., et al., 1997. Short term effects of ambient sulphur dioxide and particulate matter on mortality in 12 European cities: Results from time series data from the APHEA project. Bmj Br. Med. J. 314 (7095), 1658–1663.
Koh, W.M., Badaruddin, H., La, H., Chen, M.I.C., Cook, A.R., 2018. Severity and burden of hand, foot and mouth disease in Asia: a modelling study. Bmj Global Health 3 (1).
Leroux, B., Lei, X., Breslow, N., Leroux, B.G., 2000. Estimation of disease rates in small areas: A new mixed model for spatial dependence.
Lidia, R., Arends, et al., 2008. Meta-analysis of summary survival curve data. Stat. Med. 27 (22), 4381–4396.
MGK, A., JHR, B., 2009. An improved approximation to the precision of fixed effects from restricted maximum likelihood. Comput. Stat. Data Anal. 53 (7), 2583–2595.
Newell, K., Kartsonaki, C., Lam, K.B.H., Kurmi, O.P., 2017. Cardiorespiratory health effects of particulate ambient air pollution exposure in low-income and middle-income countries: a systematic review and meta-analysis. Lancet Planet. Health 1 (9), 368–380.
Nguyen, H.X., Chu, C., Nguyen, H.L.T., et al., 2017. Temporal and spatial analysis of hand, foot, and mouth disease in relation to climate factors: A study in the Mekong delta Region, Vietnam. Sci. Total Environ. 581, 766–772.
Requia, W.J., Adams, M.D., Arain, A., Papatheodorou, S., Koutrakis, P., Mahmoud, M., 2018. Global association of air pollution and cardiorespiratory diseases: A systematic review, meta-analysis, and investigation of modifier variables. Am. J. Public Health 108 (2), 123–130.
Ritz, J., Demidenko, E., Spiegelman, D., 2008. Multivariate meta-analysis for data consortia, individual patient meta-analysis, and pooling projects. J. Stat. Plan. Inference 138 (7), 1919–1933.

Roger, KJH., 1997. Small sample inference for fixed effects from restricted maximum likelihood. Biometrics 53 (3), 983–997.
Shah, A.S.V., Langrish, J.P., Nair, H., et al., 2013. Global association of air pollution and heart failure: a systematic review and meta-analysis. Lancet 382 (9897), 1039–1048.
Shah, A.S.V., Lee, K.K., McAllister, D.A., et al., 2015. Short term exposure to air pollution and stroke: systematic review and meta-analysis. BMJ 350, h1295.
Shang, Y., Sun, Z.W., Cao, J.J., et al., 2013. Systematic review of Chinese studies of short-term exposure to air pollution and daily mortality. Environ. Int. 54, 100–111.
Tian, Y., Liu, H., Wu, Y., et al., 2019. Association between ambient fine particulate pollution and hospital admissions for cause specific cardiovascular disease: time series study in 184 major Chinese cities. Bmj Br. Med. J. 367.
Tobler, W.R., 1970. A computer movie simulating urban growth in the detroit region. Econ. Geography 46 (2).
Viechtbauer, W., 2010. Conducting meta-analyses in R with the metafor package. J. Stat. Softw. 36 (3), 1–48.
Wu, Y., Li, S., Zhao, Q., et al., 2022. Global, regional, and national burden of mortality associated with short-term temperature variability from 2000-19: a three-stage modelling study. Lancet Planet. Health 6 (5), 410–421.
Xiao, X., Gasparrini, A., Huang, J., et al., 2017. The exposure-response relationship between temperature and childhood hand, foot and mouth disease: A multicity study from mainland China. Environ. Int. 100, 102–109.
Xing, W.J., Liao, Q.H., Viboud, C., et al., 2014. Hand, foot, and mouth disease in China, 2008-12: an epidemiological study. Lancet Infect. Dis. 14 (4), 308–318.
Yang, Z., Yang, J., Li, M., Chen, J., Ou, C.-Q., 2021. Nonlinear and lagged meteorological effects on daily levels of ambient PM2.5 and O3: Evidence from 284 Chinese cities. J. Clean. Prod. 278, 123931.
Yi, L.P., Xu, X., Ge, W.X., et al., 2019. The impact of climate variability on infectious disease transmission in China: Current knowledge and further directions. Environ. Res. 173, 255–261.
Zadnik, V., Reich, B.J., 2006. Analysis of the relationship between socioeconomic factors and stomach cancer incidence in Slovenia. Neoplasma 53 (2), 103–110.
Zhao, Q., Guo, Y., Ye, T., Gasparrini, A., Li, S., 2021. Global, regional, and national burden of mortality associated with non-optimal ambient temperatures from 2000 to 2019: a three-stage modelling study. Lancet Planet. Health 5 (7), 415–425.
Zhu, L., Wang, X.J., Guo, Y.M., Xu, J., Xue, F.Z., Liu, Y.X., 2016. Assessment of temperature effect on childhood hand, foot and mouth disease incidence (0-5 years) and associated effect modifiers: A 17 cities study in Shandong Province, China, 2007–2012. Sci. Total Environ. 551, 452–459.
Zhuang, Z.C., Kou, Z.Q., Bai, Y.J., et al., 2015. Epidemiological research on hand, foot, and mouth disease in mainland China. Viruses-Basel 7 (12), 6400–6411.